Electronic Supplementary Material (ESI) for Nanoscale.

Supporting Information

Improve alkali metal ion batteries via interlayer engineering of anodes: from graphite to graphene

Jiachen Ma,[1, #] Chen Yang,[1, 2, #] Xinjie Ma,[3] Shiqi Liu,[1] Jie Yang,[1] Linqiang Xu,[1] Jingsong Gao,[1] Ruge Quhe,[4] Xiaotian Sun,[5] Jinbo Yang,[1, 7, 8, 9] Feng Pan,[10] Xiaoyu Yang[3, 6, 11, *] and Jing Lu[1, 2, 7, 8, 9, *]

[1] State Key Laboratory for Mesoscopic Physics and Department of Physics, Peking University, Beijing 100871, P. R. China.
[2] Academy for Advanced Interdisciplinary Studies, Peking University, Beijing 100871, P. R. China.
[3] Beijing MaiGao MatCloud Technology Co. Ltd, Beijing, 100190, P. R. China.
[4] State Key Laboratory of Information Photonics and Optical Communications and School of Science, Beijing University of Posts and Telecommunications, Beijing 100876, P. R. China
[5] College of Chemistry and Chemical Engineering, and Henan Key Laboratory of Function-Oriented Porous Materials, Luoyang Normal University, Luoyang 471934, P. R. China
[6] Computer Network Information Centre, Chinese Academy of Sciences, Beijing, 100190, P. R. China
[7] Collaborative Innovation Center of Quantum Matter, Beijing 100871, P. R. China
[8] Beijing Key Laboratory for Magnetoelectric Materials and Devices, Beijing 100871, P. R. China
[9] Peking University Yangtze Delta Institute of Optoelectronics, Nantong 226010, P. R. China
[10] School of Advanced Materials, Peking University Shenzhen Graduate School, Shenzhen, 518055, P. R. China
[11] University of Chinese Academy of Sciences, Beijing,100049, P. R. China
[*] Corresponding authors: jinglu@pku.edu.cn (Jing Lu), kxy@cnic.cn (Xiaoyu Yang)

[#] These authors contributed equally to this work.

1. Van der Waals correction test

To get a more suitable van der Waals correction, a careful test is performed, taking the AB-stacked graphite and stage-I LiC_6 are taken as an example. The calculated structural parameters and the adsorption energy E_{ad} are shown in Table S1. It can be found that all the a are similar but c has a relatively large difference with the referenced value. Too small c of the AB-stacked graphite C_{12} is gained with DFT-D2, DFT-D3-BJ, optB86b, and optB88 corrections. For LiC_6, only DFT-D3-BJ correction underestimates the lattice constant c over 0.100 Å.

The adsorption energy is calculated as follows:

$$E_{\mathrm{ad}} = E_{\mathrm{LiC_6}} - E_{\mathrm{C_6}} - E_{\mathrm{Li}}$$

where $E_{\mathrm{LiC_6}}$ and E_{Li} are the total energies of LiC_6 at its equilibrium interlayer spacing and one Li atom in its bulk structure. $E_{\mathrm{C_6}}$ is half of the total energy of the AB-stacked graphite C_{12} at the equilibrium interlayer spacing (not the AA-stacked graphite with the same interlayer spacing of the corresponding LiC_6 in the main text, which leads to a difference of 0.12 eV per Li in E_{ad}). Compared with the referenced E_{ad}, DFT-D2 correction leads to a much lower E_{ad}. optB86b, optB88, optPBE and vdW-DF2 corrections lead to much higher E_{ad}.

Considering the accuracy of the calculated lattice constants and adsorption energies, the DFT-D3 correction is finally adopted.

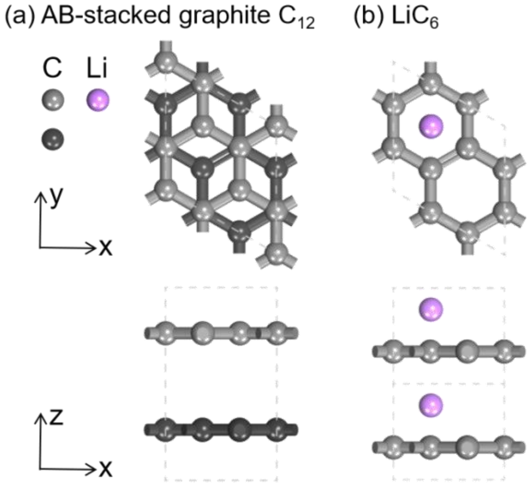

Figure S1. Top and side views of (a) AB-stacked graphite C_{12} and (b) LiC_6.

Table S1. The lattice constants (*a*, *c*) of AB-stacked graphite and LiC_6 and the corresponding adsorption energies (E_{ad}) under several commonly used van der Waals corrections. Δ*a* (Δ*c*)is the difference between the calculated *a* (c) and referenced *a* (c). The "~~strikeout~~" indicates that Δ*a* or Δ*c* is larger than 0.100 Å, or the difference of calculated E_{ad} with the referenced value is larger than 0.100 eV.

van der Waals	AB-stacked graphite C_{12}				LiC_6				E_{ad}
correction	*a* (Å)	Δ*a* (Å)	*c* (Å)	Δ*c* (Å)	*a* (Å)	Δ*a*(Å)	*c* (Å)	Δ*c* (Å)	(eV)
DFT-D2	4.266	-0.002	6.365	~~-0.406~~	4.320	0.015	3.654	-0.052	~~-0.829~~
DFT-D3	4.271	0.004	6.836	0.065	4.318	0.013	3.659	-0.047	-0.188
DFT-D3-BJ	4.271	0.003	6.651	~~-0.120~~	4.314	0.009	3.606	~~-0.100~~	-0.243
optB86b	4.272	0.004	6.550	~~-0.221~~	4.325	0.020	3.639	-0.067	~~-0.054~~
optB88	4.269	0.001	6.599	~~-0.172~~	4.323	0.018	3.678	-0.028	~~-0.065~~
optPBE	4.280	0.012	6.789	0.018	4.334	0.029	3.697	-0.009	~~-0.005~~
vdW-DF2	4.289	0.021	6.945	~~0.174~~	4.345	0.040	3.751	0.045	~~-0.018~~
Referenced value	4.268[1]	-	6.771[1]	-	4.305[1]	-	3.706[1]	-	-0.217[2]

2. AA-stacked and AB-stacked carbon layers energetic comparison

The structural illustrations of the AA-stacked and AB-stacked graphite are shown in Fig. S2(a). In the AA-stacked graphite, all C atoms in one layer are perpendicular to C atoms in the other layer, leading to a relatively strong Coulomb repulsion between neighbor carbon layers. In the AB-stacked graphite, half of the C atoms in one layer are above the center of the carbon ring in the other layer and a half are perpendicular to C atoms, which buffers the Coulomb repulsion between carbon layers, to some extend. The free energies of the carbon layers under the two stacking modes are plotted in Fig. S2(b). When the interval between layers is small, the AB-stacked graphite is more energetic stable. The most stable interval of AB-stacked graphite is 3.42 Å, with a free energy of -9.3057 eV per C atom. The most stable interval of AA-stacked graphite is 3.66 Å with a free energy of -9.3001 eV per C atom. When the interval larger than 5 Å, the interaction between the carbon layers is weakened so that the energies of the carbon layers under the two stacking modes are basically the same.

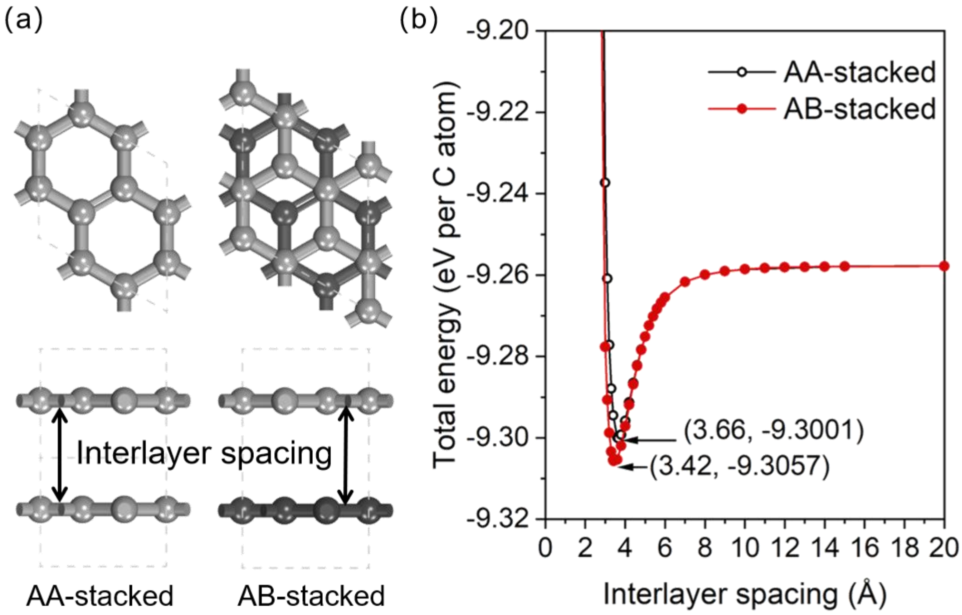

Figure S2. (a) The top views and side views of AA-stacked and AB-stacked graphite and (b) their free energies per C atom.

3. The abnormally high $N(E_f)$ of the LiC_6 structure at the interlayer spacing of 2.0 Å

To explain the abnormal high $N(E_f)$ of the LiC_6 structure at the interlayer spacing of 2.0 Å, we illustrate its band structure in Fig. S3. The band structure of LiC_6 at the equilibrium interlayer spacing of 3.7 Å is also provided for comparison.

We can find that the typical Dirac point remains in the band structure of LiC_6 at 3.7 Å. However, when the interlayer spacing of graphite decreases to 2.0 Å, the band structure has severely changed, where the Dirac point does not show. Thus, it can be speculated that the abnormally high $N(E_f)$ of the LiC_6 structure at 2.0 Å is caused by the band structure deformation with the extremely small interlayer spacing.

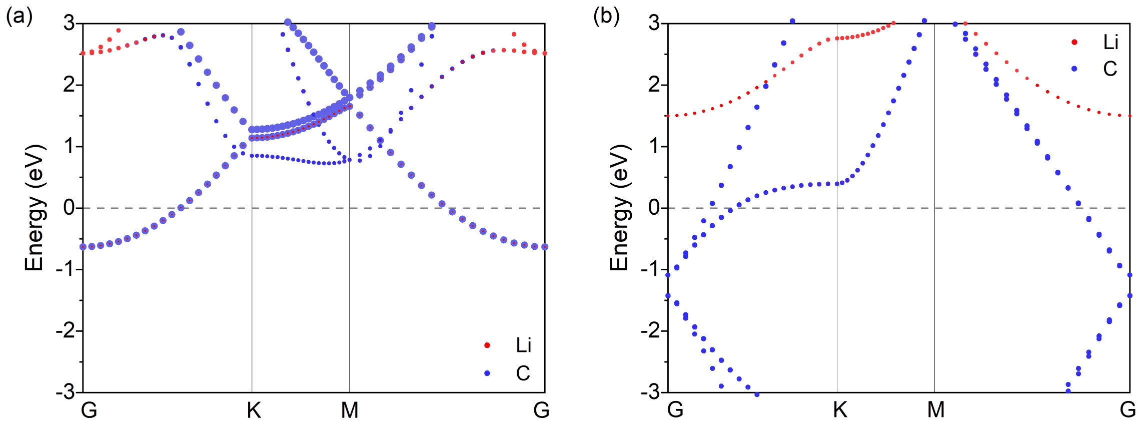

Figure S3. Band structures of LiC_6 when the interlayer spacing of graphite is at (a) 2.0 Å and (b) 3.7 Å.

4. Diffusion pathway of M ions

According to the previous studies[1, 3, 4], the "hollow-bridge-hollow" diffusion pathway is chosen, which has a lower diffusion barrier than others. The chosen diffusion pathway and the corresponding energy profiles are drawn in Fig. S4. In the initial and final images, the alkali metal ions are at two adjacent hollow sites, respectively. The intermediate images are linearly inserted, and the alkali metal ion passes through a C-C bridge. The barrier height is obtained by subtracting the lowest energy from the highest energy along the entire diffusion pathway.

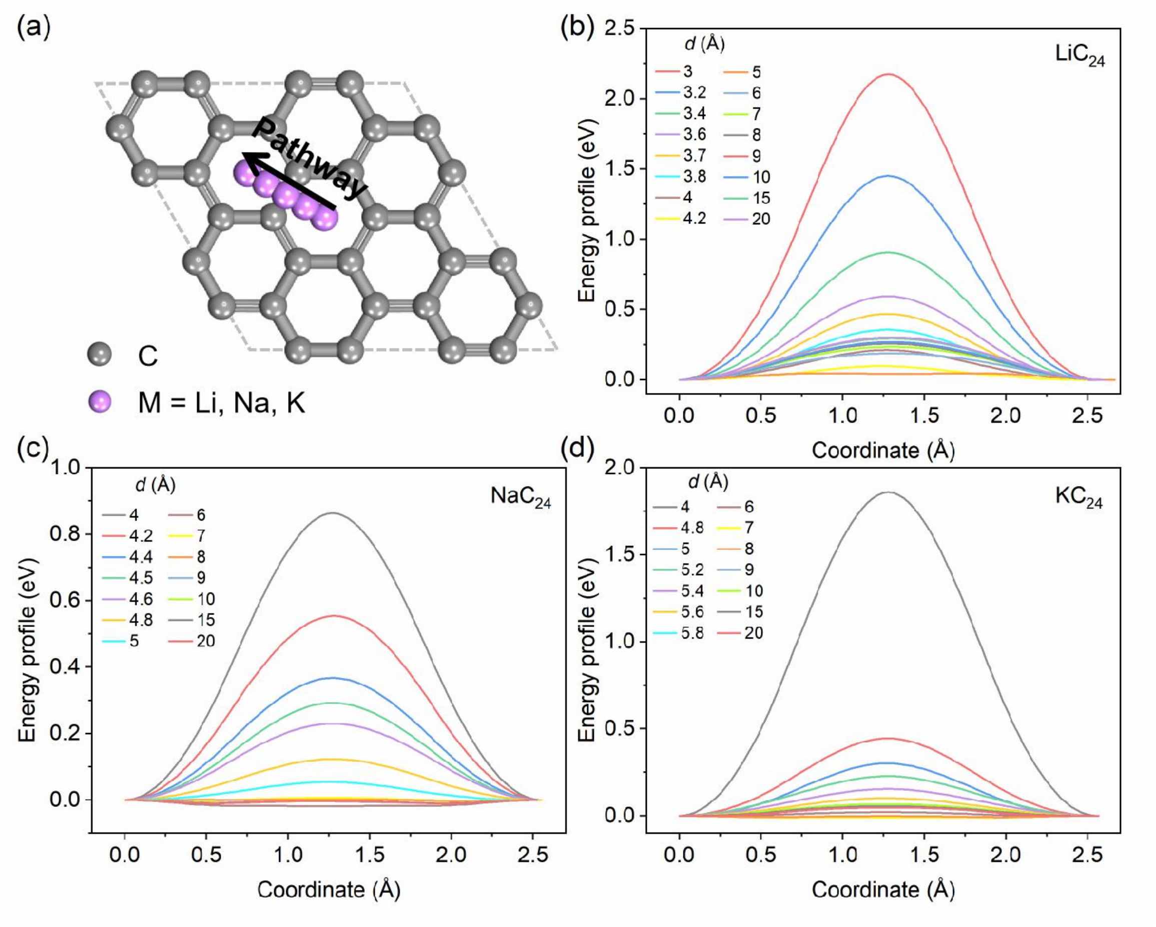

Figure S4. (a) Pathway of alkali metal ions diffusing on graphene planes and (b-c) their diffusion energy profiles at different *d*.

5. E_{ave} and OCV

E_{ave} and OCV of per $\mathrm{Li}_x\mathrm{C}$ and $\mathrm{K}_x\mathrm{C}$ unit cell at the different interlayer spacing of graphite are listed in Table S2 and Table S3. When E_{ave} becomes positive or OCV becomes negative, the maximum adsorption concentration is reached. Then the specific capacity can be obtained. In the case of large capacities, small cells are used to save computation time. In the case of small capacities, large cells are used to get a more accurate x_{max}. To make it clear, the denominators of x in Table S2 and Table S3 are the numbers of C atoms in the adopted cells. For example, for x = 10/54, the cell contains 54 C atoms. For x = 2/8, the cell contains 8 C atoms.

Table S2. E_{ave} and OCV of per $\mathrm{Li}_x\mathrm{C}$ unit cell at the different interlayer spacing of graphite. The

“~~strikeout~~” indicates that the index does not meet the corresponding criteria. The grey font represents that the capacity value is unreached.

Interlayer spacing (Å)	x	E_{ave} (eV)	OCV (V)	Capacity (mAh g^{-1})
3.0	1/54	~~0.42~~	~~-0.42~~	41
3.2	1/54	~~0.17~~	~~-0.17~~	41
3.3	9/54	0.14	0.13	372
	10/54	-0.08	~~-0.37~~	
3.4	9/54	-0.19	0.20	372
	10/54	-0.14	~~-0.33~~	
3.6	9/54	-0.23	0.27	372
	10/54	-0.18	~~-0.29~~	
3.7	9/54	-0.23	0.27	372
	10/54	-0.18	~~-0.29~~	
3.8	9/54	-0.22	0.26	372
	10/54	-0.17	~~-0.30~~	
4.0	9/54	-0.16	0.19	372
	10/54	-0.11	~~-0.35~~	
4.2	9/54	-0.06	0.07	372
	10/54	~~0.01~~	~~-0.58~~	
4.3	1/54	~~0.06~~	~~-0.06~~	41
5.0	1/54	~~0.32~~	~~-0.32~~	41
10.0	1/54	~~0.54~~	~~-0.54~~	41
15.0	1/54	~~0.55~~	~~-0.55~~	41
20.0	1/54	~~0.56~~	~~-0.56~~	41

Table S3. E_{ave} and OCV of per K_xC unit cell at different interlayer spacing. The “~~strikeout~~” indicates that the index does not meet the corresponding criteria. The grey font represents that the capacity value is unreached.

Interlayer spacing (Å)	x	E_{ave} (eV)	OCV (V)	Capacity (mAh g^{-1})
4.0	1/72	~~1.11~~	~~-1.11~~	31
4.4	1/72	~~0.31~~	~~-0.31~~	31
4.6	1/8	-0.03	0.03	279
5.0	1/8	-0.53	0.43	279
7.0	1/8	-0.44	0.44	279

	2/8	-0.03	~~-0.50~~	
8.0	2/8	-0.26	0.21	559
	3/8	~~0.35~~	~~-1.55~~	
10.0	2/8	-0.36	0.53	559
	3/8	-0.07	~~-0.51~~	
11.0	2/8	-0.30	0.42	559
	3/8	-0.19	~~-0.02~~	
12.0	3/8	-0.26	0.35	838
	4/8	~~0.007~~	~~-0.83~~	
13.0	3/8	-0.30	0.54	838
	4/8	-0.09	~~-0.52~~	
14.0	3/8	-0.28	0.54	838
	4/8	-0.16	~~-0.18~~	
15.0	4/8	-0.21	0.13	1117
	5/8	-0.01	~~-0.78~~	
16.0	4/8	-0.24	0.24	1117
	5/8	-0.09	~~-0.52~~	
17.0	4/8	-0.25	0.25	1117
	5/8	-0.14	~~-0.28~~	
18.0	4/8	-0.23	0.23	1117
	5/8	-0.18	~~-0.03~~	
19.0	5/8	-0.20	0.21	1396
	6/8	-0.08	~~-0.53~~	
20.0	5/8	-0.22	0.39	1396
	6/8	-0.12	~~-0.34~~	

6. Adsorption energies of NaC_6 and NaC_8

The adsorption energy (E_{ad}) of MC_6 and MC_8 (M = Li, Na, and K) are shown in Fig. S5. The situation of MC_6 and MC_8 are similar for each type of M. For Na, though the E_{ad} of NaC_8 is relatively smaller than that of NaC_6, their tendency is similar as the interlayer spacing increases. The lowest E_{ad} of NaC_8 is -0.19 eV per Na-ion at the interlayer spacing at 4.6 Å. But the adsorption energy becomes positive soon as the interlayer spacing enlarges. The reason why pristine carbon layers cannot adsorb Na atoms has been investigated by former research.[5, 6] They reckon that “Na has the weak binding to a given substrate” is the result of “the competition between the ionization of the metal atom and the ion-substrate coupling”. This phenomenon leads to a low capacity of less than 35 mAh·g^{-1} of Na in the graphite electrode. The capacity calculation of Na requires very large supercells (more than 100 atoms), which will consume a lot of computing resources, and the resulting capacity will be rather small and meaningless. Given that, the case of Na is not considered in the capacity calculation.

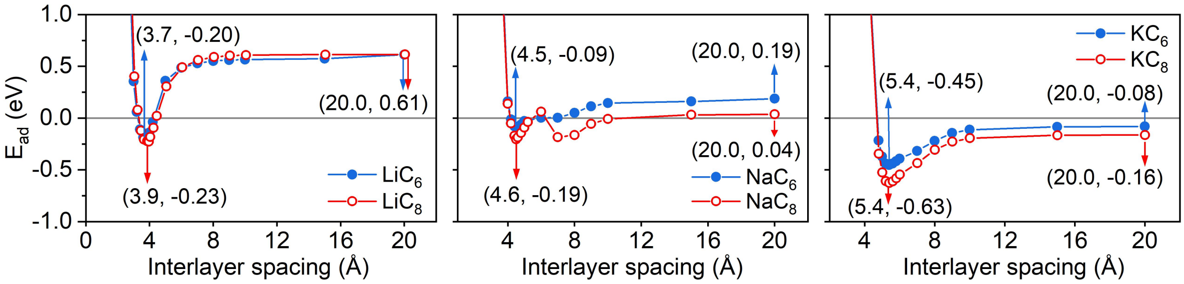

Figure S5. Adsorption energies (E_{ad}) of MC_6 and MC_8 (M = Li, Na, and K) per M ion.

7. Inner and outer interlayer spacing

On one hand, the inner interlayer spacing of 7-layered graphene is ~0.34 nm, recorded with the grazing incidence X-ray diffraction (GIXRD) pattern[7]. On the other hand, the outer interlayer spacing between 7-layered graphene and 7-layered graphene is unknown. The relationship of the “two” interlayer spacing is shown in Fig. S6. The increased K-ion storage is contributed by the enlarged outer interlayer spacing, rather than the inner one. The enlarged outer interlayer spacing corresponds to more exposed surfaces of the few-layered graphene. Although the outer one, which we focus on in the main text, is unknown, it must be larger than the intrinsic/inner interlayer spacing of graphite.

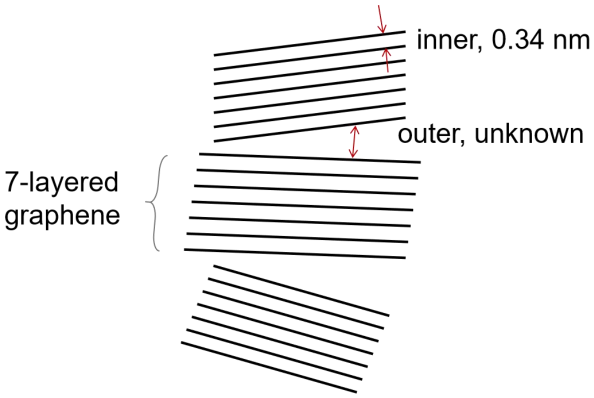

Figure S6. Schematic diagram of the "two" interlayer spacing of 7-layered graphene.

8. *Q* of three non-equivalent K_2C_8

We have considered three non-equivalent two-layered K-ions adsorbed graphene structures and provided their top views in Fig. S7. In structure A, the two layers of K ions are put on the same side of graphene. In structure B, the two layers of K ions are put on each side of graphene, and the adsorption sites are overlapping from the top view. In structure C, the two layers of K ions are put on each side of graphene, and the adsorption sites are not overlapping from the top view. According to the electron localization function, the electrons are more localized in structures B and C than in A. We also perform the Bader charge analysis to further quantitatively investigate the situation of *Q*. As listed in Table S4, compared with the situation of structure A, K atoms transfer more electrons to the carbon layer in structures B and C. Thus, when the K-ions are adsorbed on each side of the carbon layer, K-C interactions show more ionic bond properties. Since structure A has the lowest total energy, we adopt structure A in the main text.

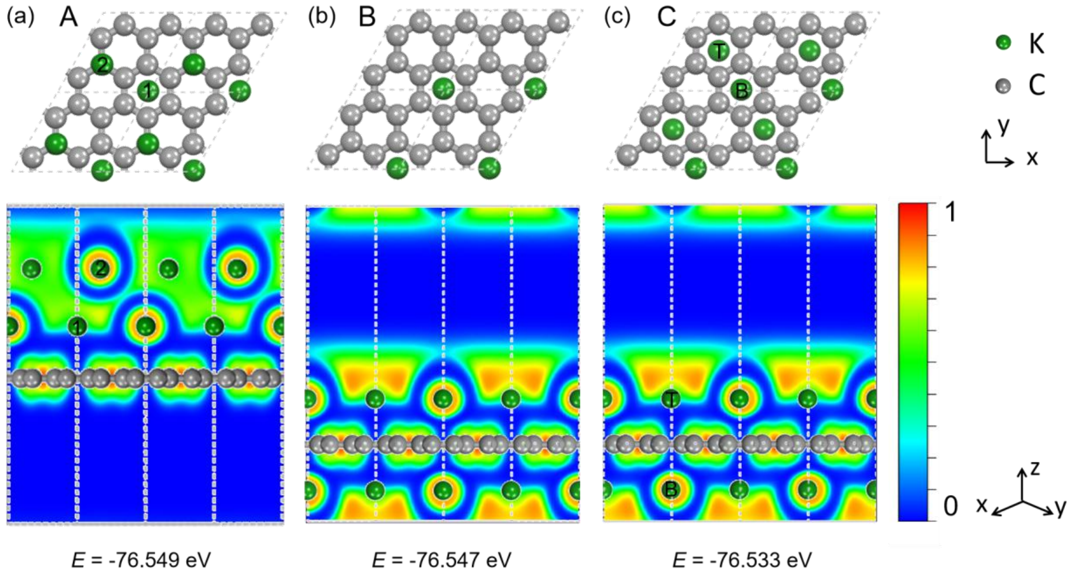

Figure S7. Top views and electron localization function (ELF) of three K_2C_8 structures.

Table S4. Transferred electrons (*Q*) from the K atoms to the C layer.

Structures	A		B		C	
K atoms	1	2	T	B	T	B
Q	0.340	-0.037	0.353	0.349	0.360	0.360

9. Adsorption of multiple layers of K-ions without external pressure

To further investigate the adsorption behavior of multiple layers of K-ions on graphite anode without external stress, we fully relax the lattice of K_xC_8 structures. Here x is equal to the K-ion layer number. The calculated E_{ave}, OCV, and enlarged d_{eq} versus d_{eq} of pristine graphite with the K layer number are shown in Fig. S8. E_{ave} keeps negative and OCV keeps positive, suggesting that the graphite anode can absorb at least five layers of K-ions. And the trend of E_{ave} and OCV seems to indicate that the adsorption can keep going without an end. However, d_{eq} of relaxed K_xC_8 increases drastically with x. Compared with that of pristine graphite (3.42 Å), d_{eq} has enlarged to 154% with one layer of K-ions (KC_8) and 271% with two layers of K-ions (K_2C_8). When graphite anode adsorbs five layers of K-ions per carbon layer, d_{eq} can even enlarge to 20.47 Å and is 599% versus that of pristine graphite. Such huge changes of d_{eq} will lead to serious volume change during the charging-discharging process in the actual case, and then poor cycling performance and even safety accidents.

Thus, we can conclude that though the adsorption of multiple K-ion layers is energetically feasible for graphite anode, the volume change is unacceptable in the actual scenarios. Interlayer engineering is needed to enlarge the interlayer spacing of the graphite anode at the very beginning.

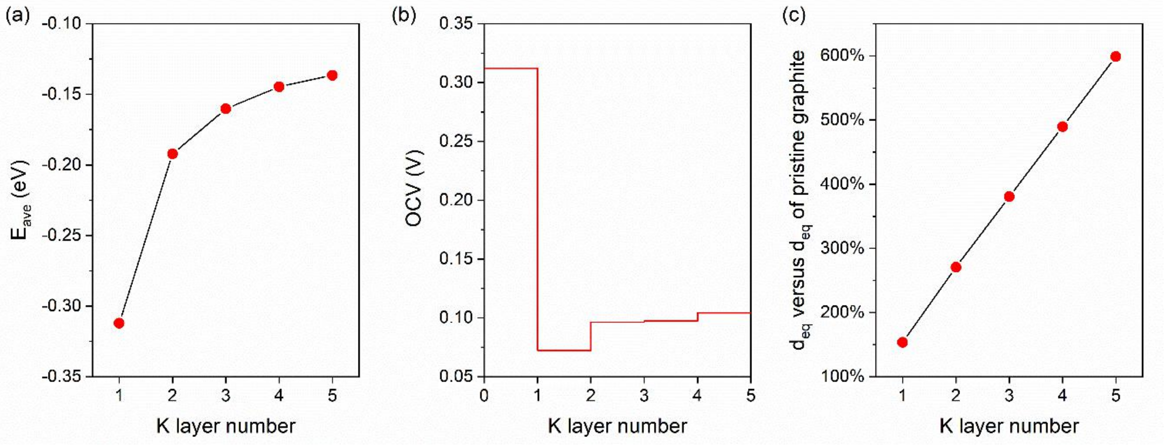

Figure S8. (a) E_{ave}, (b) OCV, and (c) enlarged d_{eq} versus d_{eq} of pristine graphite when multiple layers of K-ion intercalated into the carbon layers. The lattices of K_xC_8 structures are fully relaxed. Here x is equal to the K-ion layer number.

References

(1) S. Thinius, M. M. Islam, P. Heitjans and T. Bredow, Theoretical Study of Li Migration in Lithium–Graphite Intercalation Compounds with Dispersion-Corrected DFT Methods. *J. Phys. Chem. C* **2014,** 118, (5), 2273-2280.

(2) E. Hazrati, G. A. de Wijs and G. Brocks, Li Intercalation in Graphite: A Van Der Waals Density-Functional Study. *Phys. Rev. B* **2014,** 90, (15), 155448.

(3) K. Toyoura, Y. Koyama, A. Kuwabara, F. Oba and I. Tanaka, First-principles approach to chemical diffusion of lithium atoms in a graphite intercalation compound. *Phys. Rev. B* **2008,** 78, (21), 214303.

(4) K. Zhong, R. Hu, G. Xu, Y. Yang, J.-M. Zhang and Z. Huang, Adsorption and ultrafast diffusion of lithium in bilayer graphene: Ab initio and kinetic Monte Carlo simulation study. *Phys. Rev. B* **2019,** 99, (15), 155403.

(5) G. Yoon, H. Kim, I. Park and K. Kang, Conditions for Reversible Na Intercalation in Graphite: Theoretical Studies on the Interplay Among Guest Ions, Solvent, and Graphite Host. *Adv. Energy Mater.* **2017,** 7, (2), 1601519.

(6) K. Nobuhara, H. Nakayama, M. Nose, S. Nakanishi and H. Iba, First-Principles Study of Alkali Metal-Graphite Intercalation Compounds. *J. Power Sources* **2013,** 243, 585-587.

(7) F. J. Sonia, M. K. Jangid, M. Aslam, P. Johari and A. Mukhopadhyay, Enhanced and Faster Potassium Storage in Graphene with Respect to Graphite: A Comparative Study with Lithium Storage. *ACS Nano* **2019,** 13, (2), 2190-2204.